ISSN 0023-1584, Kinetics and Catalysis, 2020, Vol. 61, No. 4, pp. 589–594. © Pleiades Publishing, Ltd., 2020.

Hydrogen Generation by Hydrolysis of $NaBH_4$ with Efficient Co–La–Mo–B Catalyst for PEM Fuel Cells

A. Ekıncı*
Healty of School, Siirt University, Siirt, Turkey
**e-mail: aekinci@siirt.edu.tr*

Received September 12, 2019; revised November 5, 2019; accepted January 15, 2020

Abstract—In this study, Co–La–Mo–B catalyst used for hydrogen production by hydrolysis of sodium borohydride ($NaBH_4$) solution was synthesized by chemical reduction method. Characterization of the synthesized catalyst was carried out with EDX and XRD. In hydrolysis experiments, the effect of parameters such as molybdenum, NaOH and $NaBH_4$ concentration, catalyst amount and temperature were investigated. The best Mo concentration was found to be 5%. In the presence of the Co–La–Mo–B catalyst in $NaBH_4$ hydrolysis, hydrogen initial production rate was found to be 9508 mL $g^{-1}min^{-1}$. The activation energy of $NaBH_4$ hydrolyses was determined as 39.5 kJ/mol. The effect of hydrogen gas obtained using the Co–La–Mo–B catalyst in $NaBH_4$ hydrolysis on fuel cell efficiency was determined by measuring I–V values. Average efficiency values according to power and ideal voltage were found as 60 and 80%, respectively. From the results, it can be said that the Co–La–Mo–B catalyst is an ideal catalyst for PEM fuel cell applications.

Keywords: hydrogen, $NaBH_4$, hydrolysis, Co–La–Mo–B catalyst, PEM

DOI: 10.1134/S0023158420040047

INTRODUCTION

Hydrogen has been identified as one of the best alternative energy carriers to meet the growing demand for efficient and clean energy supply in the near future [1]. The use of industrial devices based on hydrogen fuel cell technology is preferred. The reason for this is that hydrogen does not require efficient storage and production environment with appropriate safety measures [2]. Hydrogen is mainly stored in metal/complex hydrides, chemically absorbed hydrogen, carbon materials, inorganic nanostructures and metal-organic structures [3–9]. Among these, sodium borohydride ($NaBH_4$) has attracted much research interest as a hydrogen storage material since the late 1990s due to its stability in alkali solutions, nonflammability, non-toxic, environmental safety and high theoretical hydrogen content [10, 11]. $NaBH_4$ hydrolysis is carried out with the following equation of reaction:

$$NaBH_4 + 2H_2O \rightarrow 4H_2 + NaBO_2. \quad \text{(I)}$$

However, NaOH is added to the $NaBH_4$ solution to control this hydrolysis reaction, i.e. to prevent its own hydrolysis reaction, and the catalyst is used to accelerate it appropriately. Thus, the catalyst is a key factor influencing the rate of H_2 production by hydrolysis of $NaBH_4$. Catalysts such as Co–B [12], Co–W–B [13], Co–Cr–B [14], Co–Fe–B [15], Co–Mo–B [16], Ni–Mo–B [17], Co–La–B [18], La–Ni–Mo–B [19], Co–La–Zr–B [20] are used in the hydrolysis of $NaBH_4$.

In this study, the effect of Co/Mo molar ratio on catalytic activity against $NaBH_4$ hydrolysis were investigated. An optimal catalyst was used to evaluate the effect of NaOH and $NaBH_4$ concentrations on hydrogen generating performance. Based on the activity at different temperatures, the activation energy of this catalytic reaction was calculated by the Arrhenius equation.

EXPERIMENTAL

Catalyst Synthesis

Co–La–Mo–B catalysts, which were not used previously in the hydrolysis of $NaBH_4$, were synthesized by chemical precipitation and reduction method. Detailed production of the catalysts is given below.

Cobalt chloride hexahydrate, lanthanum nitrate and molybdenum nitrate were added to 100 mL of pure water with a Co/La/Mo molar ratio of 7 : 3 : 5. The resulting solution was left in an ice bath to ensure that the temperature was in the range of 0–5°C and then added dropwise to a $NaBH_4$ solution (the molar ratio of $NaBH_4$ to total metal salts is 5 in 50 mL of pure water). A black precipitate was obtained. The solution

---

Abbreviations: PEM, proton exchange_membrane.

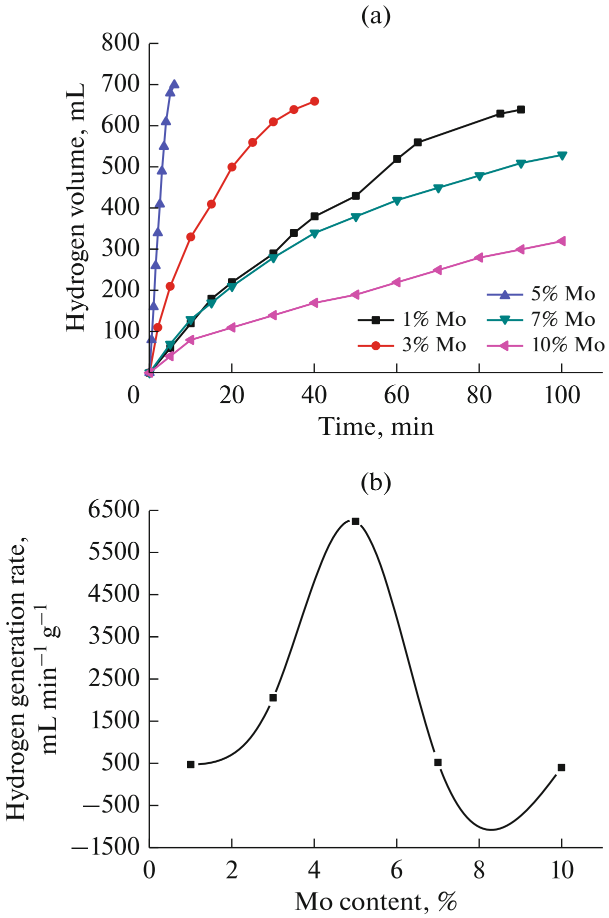

Fig. 1. (a) Hydrogen volume generated as a function of reaction time and Mo content upon hydrolysis of $NaBH_4$. (b) H_2 generation rate as a function of % Mo.

was washed several times with distilled water and ethanol to remove impurities from this precipitate. Finally, the product obtained was dried under nitrogen gas at 100°C for 8 h and the catalyst was stored in a closed container for use in the hydrolysis of $NaBH_4$.

Hydrolysis of $NaBH_4$

$NaBH_4$ hydrolysis experiments were performed in 10 mL of solution containing 25 mg of the catalyst and 2.5% of $NaBH_4$. The volume of hydrogen obtained in the hydrolysis of $NaBH_4$ was determined by the cumulative method. The effect of parameters such as Mo metal ratio, NaOH concentration, $NaBH_4$ concentration, catalyst amount and temperature was investigated. In addition, the degradation kinetics of $NaBH_4$ was determined.

PEM Fuel Cell Application

The single-cell PEM fuel cell system designed using a Pt/C catalyst in the anode and cathode portions was used for application purposes. Hydrogen produced from $NaBH_4$ hydrolysis in the presence of a Co–La–Mo–B catalyst was used in PEM fuel cell application. The measurements were carried out at 40°C with 10 mL of the solution, 25 mg of the catalyst and a resistance of 10 Ohm.

RESULTS AND DISCUSSION

$NaBH_4$ Hydrolysis

Effect of molybdenum (Mo) molar fraction. The experiments in which Mo-metal effect on the Co–La–B catalysts were investigated were carried out at 40°C with 10 mL of solution, 2.5% $NaBH_4$ concentration and 25 mg catalyst amount. The results obtained are given in Figs. 1a and 1b.

The effect of Mo concentration on catalytic activity was studied by varying the Mo molar fraction (*x*% Mo) in the Co–La–B catalyst from about 1 to 10%. As seen from Fig. 1a, when Mo concentration increases from 1 to 5%, the initial rate of hydrogen generation increases and then decreases at higher Mo concentrations. The maximum H_2 production rate (R_{max}) as a function of *x*% Mo is shown in Fig. 1b. The probable cause of this situation is that the higher Mo content in the Co–La–Mo–B catalyst may cause decomposition of the amorphous Co–La–Mo–B followed by its crystallization as metal and oxide. Another possible cause can be that the appropriate amount of metal and/or oxide in the amorphous Co–La–Mo–B catalyst helps to increase the activity for $NaBH_4$ hydrolysis, but too high metal and/or oxide content may have detrimental effects [21]. The best *x*% Mo concentration was found to be 5%, and studies were continued with this composition.

Effect of NaOH concentration. $NaBH_4$ is spontaneously hydrolyzed. At high pH values, $NaBH_4$ is stable. For this reason, it is important to examine the effect of NaOH concentration on the $NaBH_4$ hydrolysis. Experiments were performed at 40°C with 10 mL of solution, 2.5% $NaBH_4$ concentration and 25 mg catalyst amount. The results obtained are presented in Figs. 2a and 2b. When the NaOH concentration increases from zero to 2.5%, the initial rate of hydrogen production first increases and then decreases. This is probably due to the fact that the excess OH^- present in the solution has a steric effect on the hydrolysis of $NaBH_4$. However, excessive NaOH concentration results in a reduced solubility of $NaBO_2$ (a byproduct of the hydrolysis reaction). The by-product thus formed may cling to the surface of the catalyst, thereby preventing the hydrolysis reaction. The effect of other parameters was investigated in a 2.5% NaOH medium.

Effect of $NaBH_4$ concentration. Experiments in which the $NaBH_4$ effect was examined were carried out at 40°C with 10 mL of solution, 2.5% NaOH and

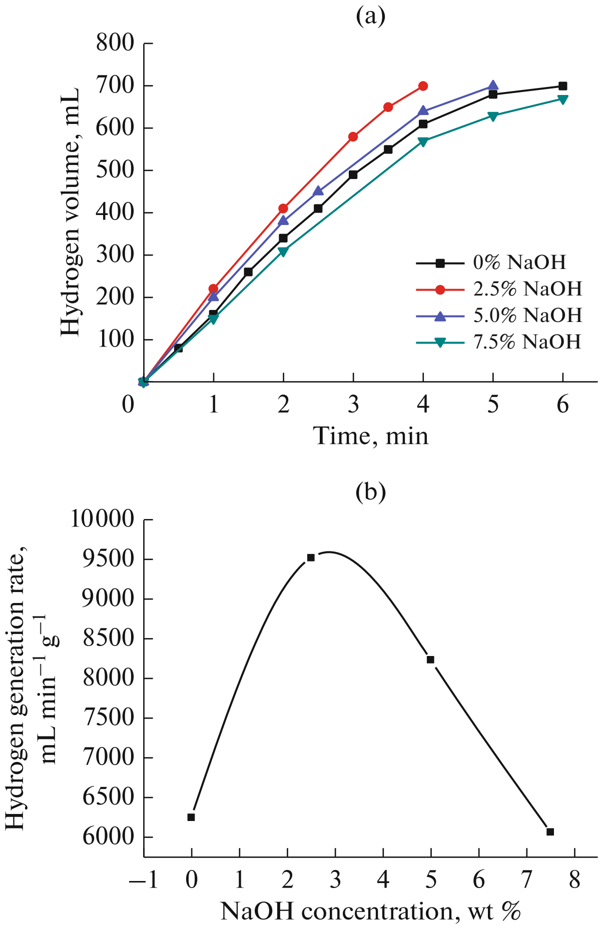

Fig. 2. (a) Hydrogen volume generated as a function of reaction time and NaOH concentration upon hydrolysis of $NaBH_4$. (b) H_2 generation rate as a function of NaOH concentration.

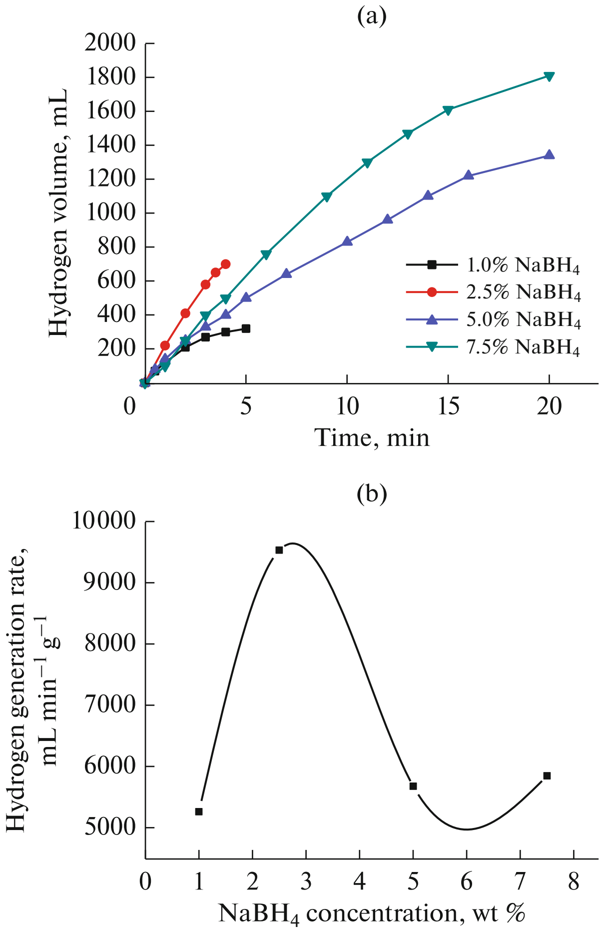

Fig. 3. (a) Hydrogen volume generated a function of reaction time and $NaBH_4$ concentration upon hydrolysis of $NaBH_4$. (b) H_2 generation rate obtained as a function of $NaBH_4$ concentration.

25 mg of catalyst. Figure 3a shows the volume of hydrogen produced as a function of time. In Fig. 3b, variation of the initial hydrogen generation rate at these $NaBH_4$ concentrations is also given. As can be seen in Fig. 3a, when $NaBH_4$ concentration increased from 1 to 2.5%, hydrogen production rate also increased. Amendola et al. [22] reported that adequate BH_4^- ions in the environment were in contact with the active zone on the catalyst surface to produce hydrogen when the concentration of $NaBH_4$ for the active catalysts increased. Moreover, it was observed that, when the concentration of $NaBH_4$ is 7.5%, the hydrogen production rate-decreased. The possible cause of this situation is that the $NaBO_2$ concentration exceeds the solubility limit. Thus, $NaBO_2$ may block the active area on the catalyst surface by precipitating [22–24]. Dependence of hydrogen production rate on alkali $NaBH_4$ solution concentration has been reported in different ways in the literature. For example, Amendola et al. [2] showed that the rate of Ru catalyzed production did not depend on $NaBH_4$ concentration. Jeong et al. [25] and Pinto et al. [26] reported that the hydrogen production rate decreased with increasing $NaBH_4$ concentration. However, Pena Alonso et al. [27] reported that hydrogen production increased more rapidly with increasing $NaBH_4$ concentration in the presence of carbon nanotube supported Pt and Pd catalyst. Patel et al. [24] showed that the hydrogen production rate increased when $NaBH_4$ concentration was low, but the hydrogen production rate remained constant at high $NaBH_4$ concentration.

Effect of catalyst amount. The effects of catalyst amount were investigated at 40°C, with 10 mL of solution, 2.5% NaOH and 2.5% $NaBH_4$ concentration (Figs. 4a and 4b). As seen from these figures, both hydrogen yield from sodium borohydride and initial production rate increase with increasing catalyst amounts. This result shows that hydrogen production from $NaBH_4$ in the presence of Co–La–Mo–B catalyst is catalyst controlled.

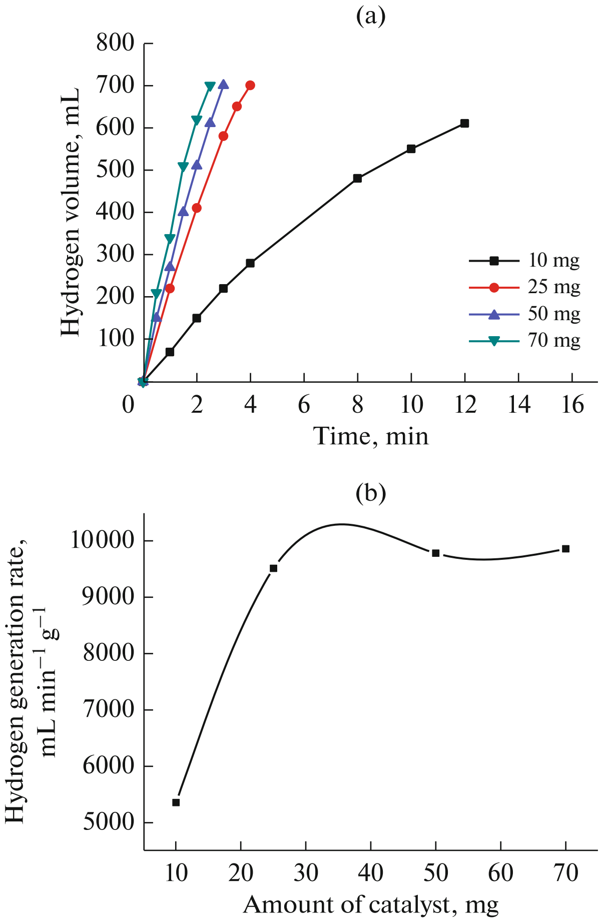

Fig. 4. (a) Hydrogen volume generated vs. time as a function of different catalyst amount upon hydrolysis of $NaBH_4$. (b) Hydrogen production rate vs. different catalyst amounts.

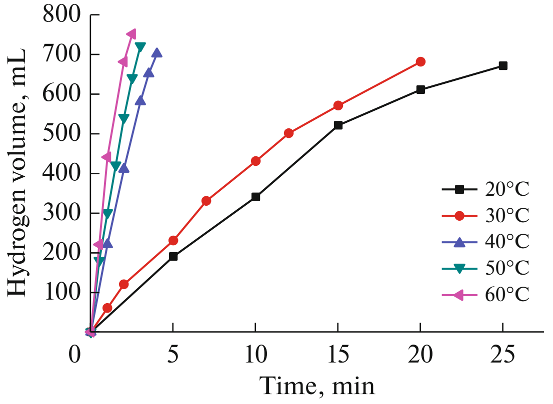

Fig. 5. Hydrogen volume generated as a function of reaction time upon hydrolysis of $NaBH_4$ solution at five different solution temperatures.

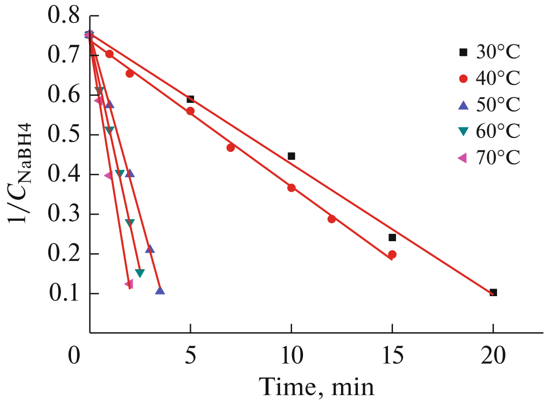

Fig. 6. Graph of $1/C_{NaBH4}$ vs. time for different temperatures.

Effect of temperature. The experiments were carried out under the conditions of 10 mL of solution, 2.5% NaOH, 2.5% $NaBH_4$ and 25 mg catalyst amount (Fig. 5). The rate of hydrolysis increases with increasing temperature. For example, hydrolysis of 2.5% $NaBH_4$ is completed at 20°C within 25 min and at 60°C within 2.5 min. The probable cause of this situation is the increase in BH_4^- ion decomposition rates due to the increasing temperature. One of the main reasons for any reaction to take place at different temperatures is to determine the reaction rate constant and the activation energy. Therefore, firstly, a reaction at the *nth* degree was used to determine the rate constants at different temperatures. The reaction rate constant for this reaction is determined by the following equation

$$\frac{1}{n-1}\left(\frac{1}{C_A^{n-1}}-\frac{1}{C_{A_0}^{n-1}}\right)=kt. \qquad (1)$$

Equation (1) can be transformed to Eq. (2)

$$\frac{1}{C_A^{n-1}}=(n-1)kt+\frac{1}{C_{A_0}^{n-1}}. \qquad (2)$$

The graph of $1/C$ vs. time for different temperatures is shown in Fig. 6. The reaction rate constants (k) for different temperatures are found from the slope of the straight lines. As shown in Fig. 6, the n value selected at all temperatures is consistent with 0.3 and all plots are linear. The catalytic reaction rate increases exponentially with increasing reaction temperature and a maximum value of 9508 mL min^{-1} g^{-1} is obtained at 333 K. The rate of catalytic hydrolysis of the alkali $NaBH_4$ solution exponentially increases with the increase in reaction temperature and a maximum value is obtained at 60°C. The temperature dependence of the rate of hydrogen production is usually expressed by the Arrhenius equation:

$$\ln k=\ln k_0-\frac{E_a}{RT}, \qquad (3)$$

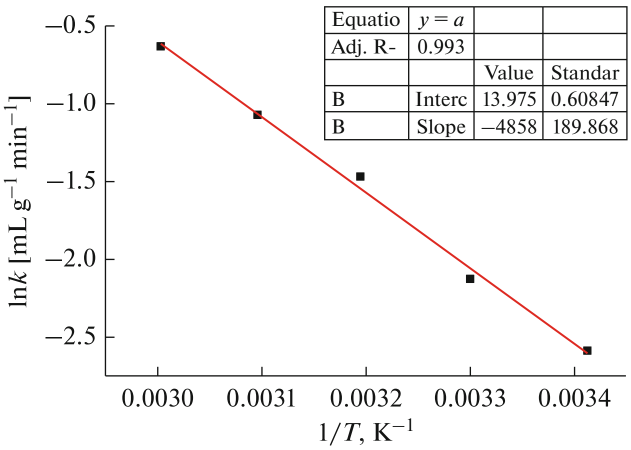

Fig. 7. Graph of $\ln(k)$ vs. $1/T$.

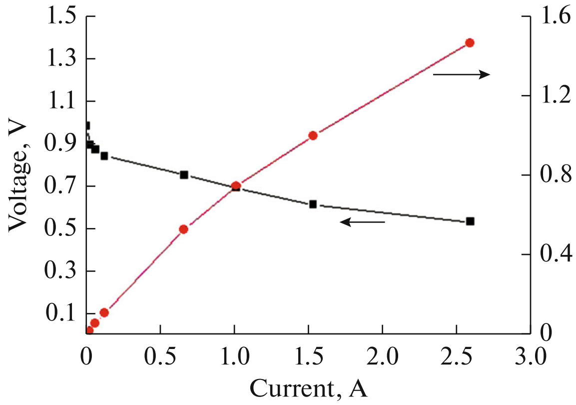

Fig. 8. Voltage–current and power–current curves.

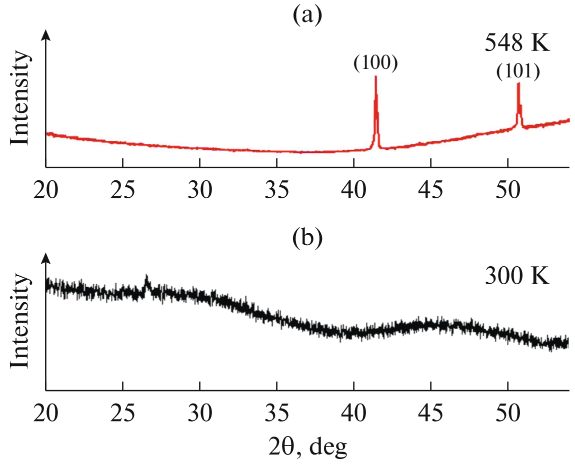

Fig. 9. XRD patterns of the Co–La–Mo–B catalyst at different temperatures, K: 548 (a), 300 (b).

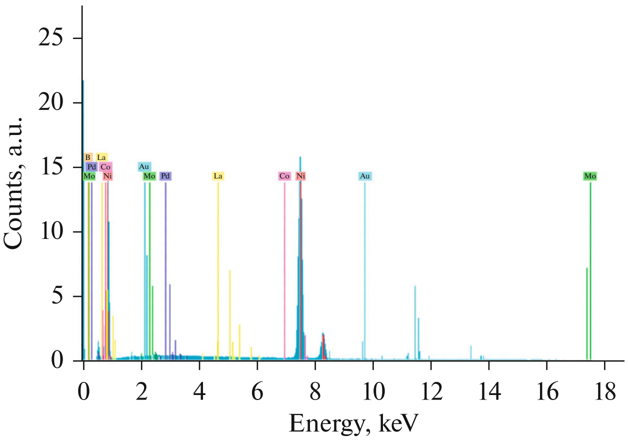

Fig. 10. EDX spectrum of the Co–La–Mo–B catalyst.

where k is the reaction rate (mL g^{-1} min^{-1}), k_0 is the reaction constant (mL g^{-1} min^{-1}), E_a is the activation energy (J/mol), R is the gas constant (8.314 J mol^{-1} K^{-1}) and T is the absolute temperature (K). The activation energy from the slope of the straight line obtained from the graph of $\ln(k)$ vs. $1/T$ shown in Fig. 7 was calculated as 39.5 kJ/mol. Compared to the activation energies calculated in the previous studies, Co–B (68 kJ/mol) [12], Co–La–B (42.4 kJ/mol) [18], Co–La–Zr–B (60.06 kJ/mol) [20], it can be said that the catalyst we synthesized demonstrates higher activity.

PEM fuel cell application of catalyst. Hydrogen produced from $NaBH_4$ hydrolysis in the presence of Co–La–Mo–B catalyst was used in PEM fuel cell application. The values used for the measurement are temperature—40°C, solution volume—10 mL, catalyst amount—25 mg, resistance—10 Ohm. Graphical analysis of the measurements were performed. The current–voltage–power curves showing the PEM fuel cell performance values for the catalyst are also indicated in Fig. 8. The efficiency value according to the power is 60%, while the efficiency value according to the ideal voltage is 80% [28, 29].

Catalyst characterization. Figure 9 indicates XRD patterns of the Co–La–Mo–B catalyst. According to XRD diffraction patterns taken at 548 K, the (100) and (101) planes of the hexagonal close packed (HCP) Co phase were detected, and the sharp peaks explained that Co electrodeposit has a crystalline structure. However, an XRD diffraction pattern taken at 300 K demonstrates that the Co–La–Mo–B catalyst is amorphous. XRD analysis revealed that the temperature of XRD plays an important role to change structure of catalyst from polycrystalline to amorphous.

The chemical composition of the Co–La–Mo–B catalyst was determined by EDX. Figure 10 indicates that Co, La, Mo and B elements can be detected.

CONCLUSIONS

In this study, a Co–La–Mo–B catalyst was prepared by chemical reduction and precipitation method. The maximum hydrogen production by volume was observed when 5% of Mo was added. Catalytic activities were measured for different $NaBH_4$ concentrations, NaOH concentrations, catalyst amounts and reaction temperatures. The volume of hydrogen produced was found to increase gradually with increasing $NaBH_4$ concentration from 1 to 7.5 wt %. However, when the $NaBH_4$ concentration was 2.5%, the hydrogen production rate was found to be 9508 mL g^{-1} min^{-1}. The effects of the NaOH concentration are similar to that of $NaBH_4$ concentration, whereas the hydrogen production rate reaches its maximum value when the NaOH concentration reaches 2.5 wt %. It was determined that the hydrogen production rate increased with increasing amount of the catalyst. It has been determined that with increasing temperature, the hydrogen production rate has increased significantly especially from 40°C. Based on the relationship between $\ln k$ and $1/T$ from the reaction dynamics equation, the value of activation energy in the presence of the Co–La–Mo–B catalysts was calculated as 39.5 kJ/mol. This value was compared with previous studies. In PEM fuel cell application, average efficiency values according to power and ideal voltage were found as 60 and 80%, respectively. From the results, it can be said that the Co–La–Mo–B catalyst is an ideal catalyst for PEM fuel cell applications.

REFERENCES

1. Graetz, J., *Chem. Soc. Rev.*, 2009, vol. 38, no. 1, p. 73.
2. Amendola, S.C., Sharp Goldman, S.L., Janjua, M.S., Kelly, M.T., Petillo, P.J., and Binder, M., *J. Power Sources*, 2000, vol. 85, no. 2, p. 186.
3. Cheng, F., Ma, H., Li, Y.M., and Chen, J., *Inorg. Chem.*, 2007, vol. 46, no. 3, p. 788.
4. Holladay, J.D., Wang, Y., and Jones, E., *Chem. Rev.*, 2004, vol. 104, no. 10, p. 4767.
5. Noh, J.S., Agarwal, R.K., and Schwarz, J.A., *Int. J. Hydrogen Energy*, 1987, vol. 12, no. 10, p. 693.
6. Ogden, J.M., Steinbugler, M.M., and Kreutz, T.G., *J. Power Sources*, 1999, vol. 79, no. 2. p. 143.
7. Schlapbach, L. and Zuttel, A., *Nature*, 2001, vol. 414, no. 6861, p. 353.
8. Wang, J., Ebner, A.D., and Ritter, J.A., *J. Phys. Chem. C*, 2007, vol. 111, no. 40, p. 14917.
9. Züttel, A., *Mater. Today*, 2003, vol. 6, no. 9, p. 24.
10. Santos, D.M.F., and Sequeira, C.A.C., *Renewable Sustainable Energy Rev.*, 2011, vol. 15, no. 8, p. 3980.
11. Schlesinger, H.I., Brown, H.C., and Hyde, E.K., *J. Am. Chem. Soc.*, 1953, vol. 75, no. 1, p. 209.
12. Liu, B.H., Li, Z.P., and Suda, S., *J. Alloys Compd.*, 2006, vol. 415, no. 1, p. 288.
13. Ekinci, A., Sahin, O., Saka, C., and Avci, T., *Int. J. Hydrogen Energy*, 2013, vol. 38, p. 15295.
14. Baytar, O., *Acta Chim. Slov.*, 2018, vol. 65, no. 2, p. 407.
15. Patel, N., Fernandes, R., and Miotello, A., *J. Catal.*, 2010, vol. 271, no. 2, p. 315.
16. Fernandes, R., Patel, N., Miotello, A., Jaiswal, R., and Kothari, D.C., *Int. J. Hydrogen Energy*, 2011, vol. 36, no. 21, p. 13379.
17. Wang, W.-y., Yang, Y.-q., Luo, H.-a., and Liu, W.-y., *Catal. Commun.*, 2010, vol. 11, no. 9, p. 803.
18. Chang, J. and Du, F.L., *Adv. Mater. Res.*, 2013, vols. 724–725, p. 735.
19. Sahin, O., Ekinci, A., Balbay, A., and Saka, C., *Surf. Eng.*, 2017, vol. 33, no. 7, p. 499.
20. Loghmani, M.H. and Shojaei, A.F., *J. Alloys Compd.*, 2013, vol. 580, p. 61.
21. Ding, X.-L., Xianxia, Y., Jia, C., and Ma, Z.-F., *Int. J. Hydrogen Energy*, 2010, vol. 35, no. 20, p. 11077.
22. Amendola, S.C., Janjua, M.S., Goldman, S., and Spencer, N.C., *Int. J. Hydrogen Energy*, 2000, vol. 25, no. 10, p. 969.
23. Ingersoll, J.C., Mani, N., Thenmozhiyal, J.C., and Muthaiah, A., *J. Power Sources*, 2007, vol. 173, no. 1, p. 450.
24. Patel, N., Fernandes, R., and Miotello, A., *J. Power Sources*, 2009, vol. 188, p. 411.
25. Jeong, S.U., Kim, R.K., Cho, E.A., Kim, H.J., Nam, S.W., Oh, I.H., Hong, S.A., and Kim, S.H., *J. Power Sources*, 2005, vol. 144, no. 1, p. 129.
26. Pinto, A.M.F.R., Falcao, D.S., Silva, R.A., and Rangel, C.M., *Int. J. Hydrogen Energy*, 2006, vol. 31, no. 10, p. 131.
27. Pena-Alonso, R., Sicurelli, A., Callone, E., Carturan, G., and Raj, R., *J. Power Sources*, 2007, vol. 165, no. 1, p. 315.
28. Amendola, S.C., Sharp-Goldman, S.L., Janjua, M.S., Spencer, N.C., Kelly, M.T., Petillo, P.J., and Binder, M., *Int. J. Hydrogen Energy*, 2000, vol. 25, p. 969.
29. *Handbook of Fuel Cells, Fundamentals Technology and Applications*, Vielstich, W., Lamm, A.G.H., and Gasteiger, H.A., Eds., Electrocatalysis, Hoboken: Wiley, 2003, vol. 2.